Thermochimica Acta, 77 (1984) 341–356
Elsevier Science Publishers B.V., Amsterdam – Printed in The Netherlands

THERMOLYSIS OF POTASSIUM TETRAPEROXOCHROMATE(V). I. ISOTHERMAL CONDITIONS

V.V. SVIRIDOV, A.I. LESNIKOVICH, S.V. LEVCHIK, K.K. KOVALENKO and V.G. GUSLEV

Institute of Physico-Chemical Problems, Byelorussian State University, Minsk 220080 (U.S.S.R.)

(Received 20 January 1984)

ABSTRACT

The thermolysis of K_3CrO_8 is characterized by autocatalytic-kinetics and the mean values of effective Arrhenius parameters are $E = 69 \pm 12$ kJ mol^{-1}, $\log A = 7 \pm 2$ s^{-1}. Mass spectrometer, microscopic, X-ray diffraction and particularly ESR-sprectroscopic studies, as well as specific surface measurements, have led to the conclusion that K_3CrO_8 thermolysis is characterized by nuclei multiplication through the entire crystal bulk. Defects in the crystal volume appearing in the induction period of thermolysis or in γ-irradiated K_3CrO_8 make the most important contribution to nucleation. K_3CrO_8 is found to be promising as a model object in topochemistry.

INTRODUCTION

Potassium tetraperoxochromate(V), K_3CrO_8, is attractive for the unusual composition of the anion formed by a pentavalent chromium atom and four peroxide groups [1–7] as well as for its ability to generate singlet oxygen in solutions [8] (but not during solid-phase decomposition [9]). Despite the fact that chromium is in a valence state untypical of this element and peroxide groups coexist in the CrO_8^{3-} anion, potassium tetraperoxochromate is a rather stable substance although it is subjected to deep radiolysis and photolysis [10].

Because of pentavalent chromium this compound is paramagnetic. The ESR spectrum of matrix-isolated ions of CrO_8^{3-} [7,11] and polycrystal K_3CrO_8 [3,4] has the form typical of paramagnetic centres ($S = 1/2$) with an axially symmetric g-factor tensor. The line in the ESR spectrum of this salt has the Lorentz form due to the exchange interaction. In contrast to an overwhelming majority of paramagnetic salts, paramagnetism of K_3CrO_8 is caused by the anion component of the lattice, i.e., by the part of the salt which undergoes chemical changes in the reactions of decomposition of such compounds formed by a simple cation and multi-atomic anion. As the anion state in tetraperoxochromate may be characterized using the high-senstivie

0040-6031/84/$03.00

ESR method, this salt appears to be of interest in studying the specificities of the solid-phase reactions [12] and differs advantageously from similar K_3NbO_8 and K_3TaO_8 salts previously studied [13]. The aim of the present work is to elucidate these specificities using various methods of studying and affecting the substance, which is regarded reasonable in solving similar problems [14].

EXPERIMENTAL

The thermal decomposition of K_3CrO_8 was studied, which has been prepared using the methods of Brauer [15] and which has been identified with the help of X-ray diffraction investigations. The $g_{\|}$ and $g_{\perp}$ values of the ESR spectrum coincided with those previously described [16]. CrO_3 (pure for analysis), KOH (chemically pure) and hydrogen peroxide (especially pure) were used for synthesis. Samples were synthesized repeatedly. Changes in sample preparation which were difficult to control, affected its appearance and chemical composition. Samples produced under the same conditions differed in colour and dispersion. These samples were mainly small red-brown crystals. With synthesis performed at temperatures lower than those indicated in ref. 15, the crystals grow more slowly to become larger in size, some of them (the largest ones) having a blue-violet metal colour that becomes more intense with storing. Some of the samples were washed with icy water, others with 97% alcohol and dry ether. Washing with water was performed to prevent possible effects of organic substances on the course of the processes under study. However, samples washed with water and dried at 325 K were lighter in colour than those washed with alcohol and ether, and their particles had no regular shape, intrinsic in K_3CrO_8 particles. These samples were not therefore used in the experiment. The samples obtained are fairly stable in storage. The storage of the sample for 3 months in a dark excicator did not affect its chemical composition; it decomposed partly after 14 months of storage. Some of its crystals had yellow chromate spots under microscope examination.

It has been suggested [17] that perchromates can be analysed by the amount of oxygen generated during their decomposition in an acid solution

$$2\ CrO_8^{3-} + 12\ H^+ \rightarrow Cr^{3+} + H_2O + 5\ O_2$$

But they are partially decomposed by the following equation

$$4\ CrO_8^{3-} + 2\ H_2O \rightarrow 4\ CrO_4^{2-} + 4\ OH^- + 7\ O_2$$

describing CrO_8^{3-} decomposition in a neutral solution. In the present experiments, as oxygen ceased to be generated and its volume was measured, the solution was boiled to remove the dissolved oxygen residues. The amount of chromate was determined iodometrically. The allowance for two ways of

K_3CrO_8 decomposition permitted a more accurate chemical analysis.

Thermal decomposition was performed in 10^{-4} N m^{-2} vacuum at 400–425 K (± 0.2). Four to five tests were run at each fixed temperature. Insignificant gas release in the nonisothermal region was ignored. As thermolysis of K_3CrO_8 may be accelerated due to self-heating and its crystals are scattered during splitting, in order to avoid local superheating and losses of the substance, therefore, a small 20–30-mg portion of fine-crystal (< 50 μm) salt was uniformly distributed over the bottom of the pan of a quartz spring balance (of 0.08 mg/division sensitivity) and covered by quartz wool from above. For control, kinetic curves were obtained by registering gas release using the device equipped with a McLeod manometer. Samples diluted with an inert substance were also used. The time-of-flight mass spectrometer MCX-4 with the system of immediate sample supply into the ionization chamber was employed. In the latter case, the substance (some tens of 10–20 μm crystals) was placed between the two titanium plates of the low-inertia band heater and decomposition proceeded under isothermal conditions maintained by a programmed thermoregulator. In the course of thermal decomposition, the specific surface of the samples (at different thermal decomposition stages) was measured in accordance with the crypton adsorption at 77 K. The samples were thermally decomposed in an adsorption plant. Interruptions in thermal decomposition necessary for measuring the specific surface amounted to 4–5 h. As preliminarily discovered, even longer breaks in vacuum did not affect thermal decomposition; therefore, the results of specific surface measurements may be related immediately to the points on the kinetic thermal decomposition curve where it was interrupted.

The observations of thermolysis development under an optical microscope (with $\times 200$ magnification) were performed using a large-crystal (up to 1 mm long) sample. The sample was placed in a special cell. The walls of the cell were plane-parallel with a gap of no more than 1 mm. The cell was thermostatted within ± 1 K. The crystals under study were placed near the controlling thermocouple junction. Thermolysis was performed under vacuum with continuous pumping out of the thermolysis products. Since the test crystals were rather large and scattered when being split during thermolysis, the decomposition of a single crystal was not observed, but the total qualitative picture of thermolysis was obtained.

The ESR spectra were recorded at room temperature using an E-12 spectrometer with high-frequency magnetic field modulation at 3.2-cm wavelength. To avoid the effect of atmospheric gases, the decomposition products were studied in an evacuated ampule. The area, A, under the ESR signal curve proportional to the quantity of paramagnetic centres was calculated by the method of odd moments for assymetric lines [18] and related to the maximum area, A_{max}, for the given kind of centres.

The K_3CrO_8 decomposition residue was roentgenographically identified on the diffractometer DPOH-2. To do this, the substance was thermolysed at

403 K on the slide in the air thermostat with P_2O_5 moisture absorber. After thermal decomposition the sample was immediately covered with nitrocellulose varnish.

K_3CrO_8 was preliminarily irradiated with ultraviolet light in an evacuated quartz vessel using a powerful 1 kJ s^{-1} mercury-vapour lamp placed 25 cm away from the sample. The temperature within the irradiation region was kept within 295 ± 1 K. γ-Irradiation was performed by the ^{60}Co source of 340 r s^{-1} power at room temperature. Samples were irradiated in evacuated glass ampules. The radiolysis degree was determined through chemical analysis of the samples.

RESULTS AND DISCUSSION

Chemical analysis of three K_3CrO_8 samples synthesized under equal conditions has shown the amount of "active" oxygen in them to be between 97.1 and 99%, and that of chromium between 105 and 101.6% the calculated quantity. K_2CrO_4, being used for K_3CrO_8 synthesis, is probably the dominating admixture in K_3CrO_8. The data of chemical analysis support this assumption. Later, the purest samples were employed containing 99% oxygen and 101.5% chromium, which approximately corresponds to 1% K_2CrO_4 admixture.

The amount of oxygen released during thermolysis and X-ray diffraction (Fig. 1) confirm the following conventional scheme of thermal decomposition

$$K_3CrO_8 \rightarrow K_2CrO_4 + KO_2 + O_2$$

Note, however, that some lines in Fig. 1 are still to be identified.

The kinetic curves of K_3CrO_8 thermolysis are sigmoid (Fig. 2) and linearize in the coordinates of the auto-catalytic reaction equation (Fig. 3). The large addition of inert material (Al_2O_3) showed that the shape of the kinetic curve could not be attributed to the self-heating of the substance. The Arrhenius dependence of this reaction rate constant is presented in Fig. 4: $E + 69 \pm 12$ kJ mol^{-1}, $\log A = 7 \pm 2$ s^{-1}. In the coordinates of the equation $\alpha = 1 - \exp(-k\tau^n)$ with $\alpha = 0.02$–0.9 straight lines with $n > 5$ are obtained. The value of $E \approx 59$ kJ mol^{-1} corresponds to the above main section of kinetic curve anamorphosis. The sigmoid kinetic curve may be described by the following equation including two constants

$$\frac{d\alpha}{d\tau} = k_1(1 - \alpha) + k_2\alpha(1 - \alpha)$$

The values of E and $\log A$ found for k_1 and k_2 were 52 ± 12, 5 ± 2 and 67 ± 12, 7 ± 2, respectively, i.e., they coincided within the errors and the representation of the entire decomposition stage in terms of a single rate constant and E and A (Fig. 4) seem to be valid.

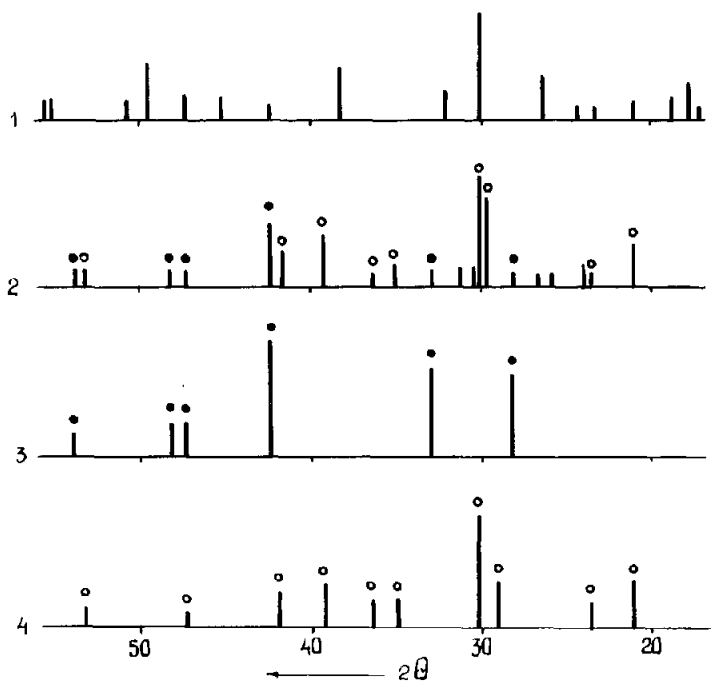

Fig. 1. Dashed roentgenograms of K_3CrO_8 and its thermolysis products: 1, K_3CrO_8; 2, products of K_3CrO_8 thermolysis at 403 K; 3, KO_2; 4, K_2CrO_4.

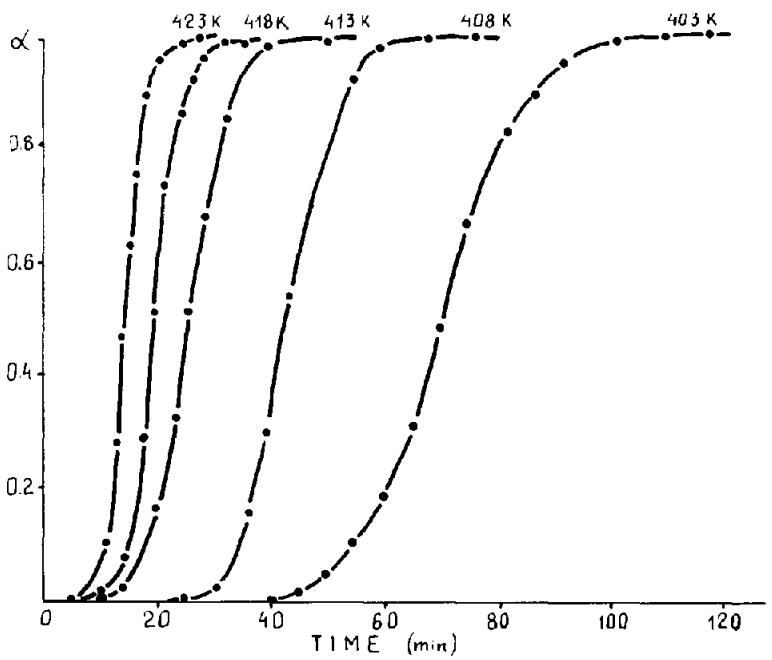

Fig. 2. Kinetic curves of thermal K_3CrO_8 decomposition.

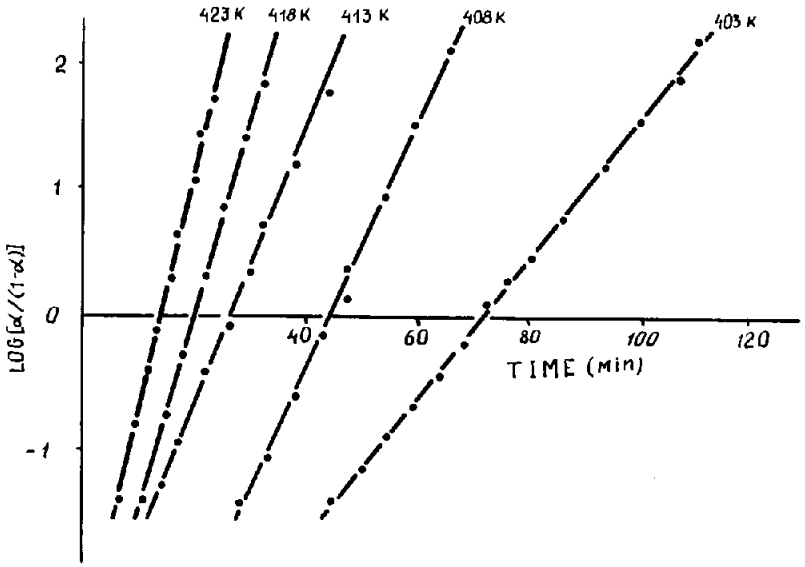

Fig. 3. Linearized form of kinetic K_3CrO_8 thermolysis curves.

It is known [14] that a formal kinetic description does not provide a good basis for the identification of the mechanism of a solid-phase reaction, and, although Fig. 3 indicates possible nucleation according to Prout–Thompkins, we have endeavoured to reveal the main features of K_3CrO_8 thermolysis using direct methods.

A mass spectrometer study of a small amount of crystals has shown that their decomposition at 408 K is a sum of weak explosion-like O_2 ejections

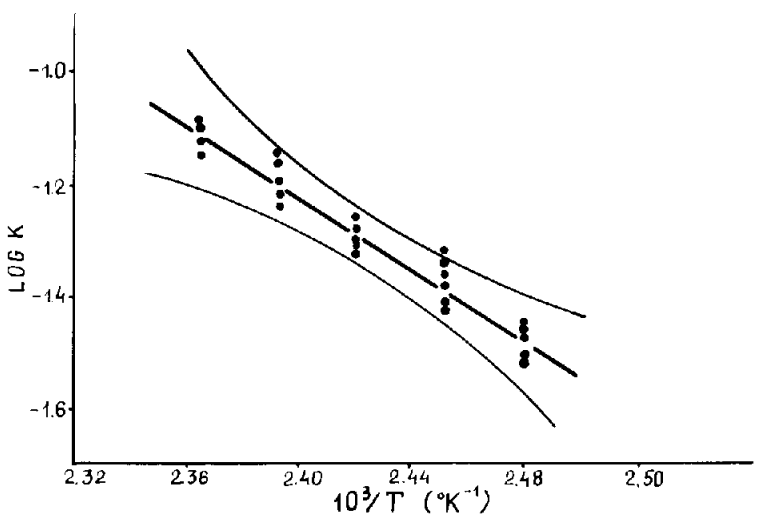

Fig. 4. Arrhenius dependence of thermal K_3CrO_8 decomposition rate constants.

recorded against a more uniform background of generation of this product. However, summation of O_2 peak intensities at one and the same τ value performed by the data of five experiments yields the total kinetic curve which at $\alpha < 0.5$ does not practically differ from that obtained at the same temperature using the conventional method. These tests manifest that the total kinetics is determined not only by the mechanism of the process at the microscopic level, but also by such macrofactors as crystal splitting and their asynchronous changes.

Microscopic observations have evidenced that initial crystals glittering in reflected light and transparent in transmitted light (Fig. 5) become dull and opaque after short-time heating (10–20 min at 403 K). After 30–40 min some crystals start to split and scatter. The process of transverse stripe formation on crystals (Fig. 6) also points to the onset of enhanced decomposition (see the kinetic curve). With further decomposition (50–90 min), crystals are fragmented or cracks are formed along these stripes, the places of splits being orange-yellow in colour. A completely decomposed crystal is bright yellow, cracked, with slightly rounded crack edges (Fig. 7).

Measurements of the specific surface during K_3CrO_8 decomposition at 405 K provided the following mean values ($m^2\ g^{-1}$): 0.18 for the initial sample; 0.55 at the end of the induction period; 2.12 at the maximum rate point; 0.4 after complete decomposition. Thus, at the end of the induction period the specific sample surface is 3 times that of the initial sample, and it shows a 12-fold increase in the vicinity of the maximum rate. Microscopic observations permit to attribute surface changes to partial splitting of small

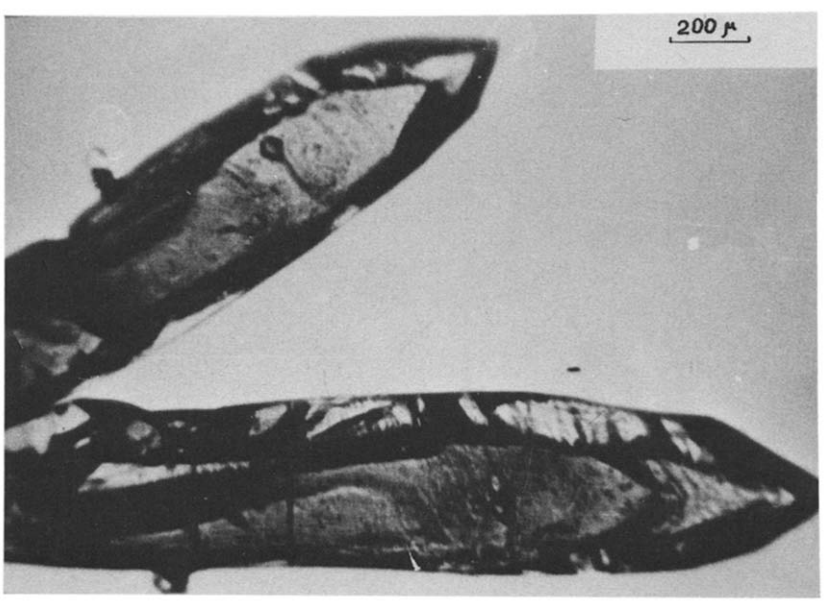

Fig. 5. Nondecomposed K_3CrO_8 crystal.

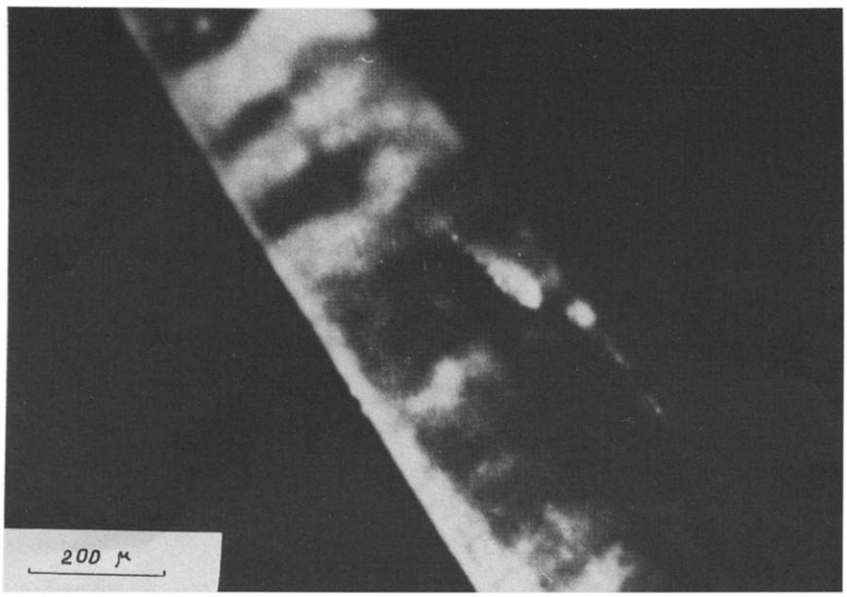

Fig. 6. K_3CrO_8 crystal at the beginning of enhanced decomposition.

crystals at the end of the induction period and to their further disintegration in the course of thermal decomposition. As decomposition ends, particles of the decomposition products grow, defects are healed and the specific surface starts to decrease.

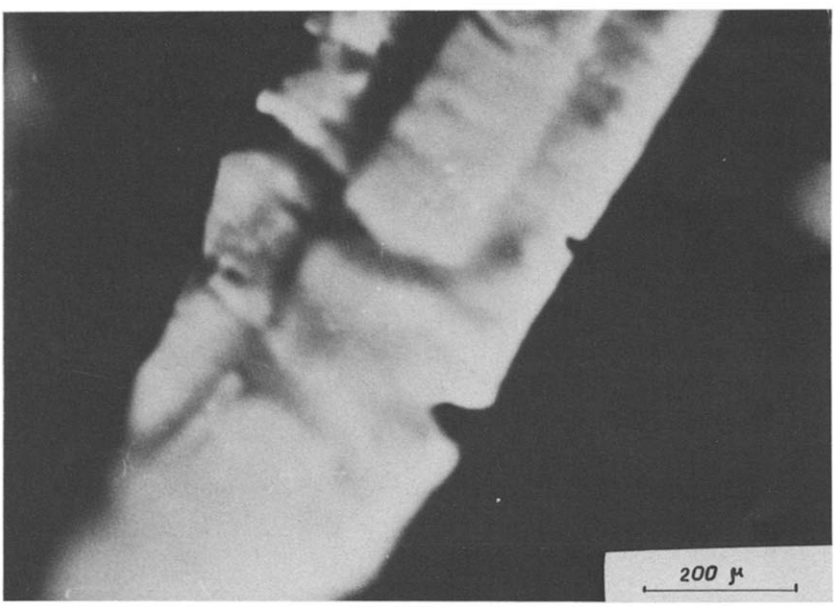

Fig. 7. Completely decomposed K_3CrO_8 crystal.

All these facts do not contradict the assumption on the decomposition in accordance with the mechanism of nuclei multiplication. They also demonstrate that the multiplication process is not only confined to the crystal surface but penetrates into the bulk of the crystal.

Further detailed investigation of the thermolysis picture was performed using the ESR method. The initial sample spectrum is given in Fig. 8. After 4 min heating at 403 K the line broadens and becomes more symmetric, the basic g-factor value remaining constant. This fact indicates a decrease in the anisotropy parameter due to broadening of the individual line of some crystals. This change of the line shape enhances as the time of heat treatment increases to the end of the induction period, and the line becomes almost symmetric (Fig. 9). As it is seen from Fig. 10, the intensity of the ESR signal of K_3CrO_8 sharply decreases in the first minutes of heating. At $\alpha \approx 0.1$ a narrow anisotropic signal (Fig. 9, curve 6; Fig. 11A, B) appears against the background of the line indicated above. The intensity of this signal passes through a maximum at $\alpha \approx 0.8$ (Fig. 10).

Following the constant g-factor, it is natural to conclude that at different decomposition stages the same paramagnetic centres are observed in K_3CrO_8, these being CrO_8^{3-} anions. Therefore, the line broadening may be attributed to a disturbance in the exchange interaction in the system of these ions which broadens the initial salt line to the value determined by the dipole–dipole interaction. The disturbance of the spin exchange interaction may be caused by the growing symmetry of the Cr(V) ion environment due, for example, to the formation of CrO_4^{3-}, or by oxidating–reducing CrO_8^{3-} ion changes including changes in the valent state of chromium. Processes of this kind taking place in the induction period and leading both to line broaden-

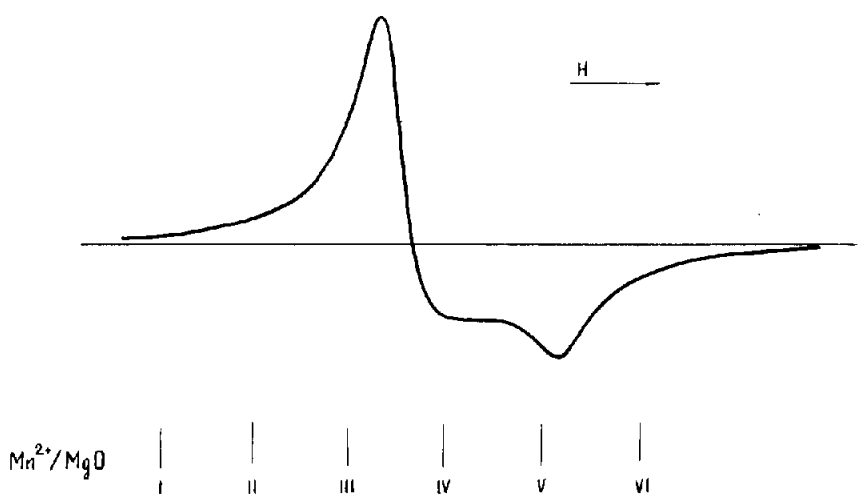

Fig. 8. ESR spectrum of K_3CrO_8. At and below I–VI, numbers of the Mn^{2+} line are for the Mn^{2+} sample in MgO lattice.

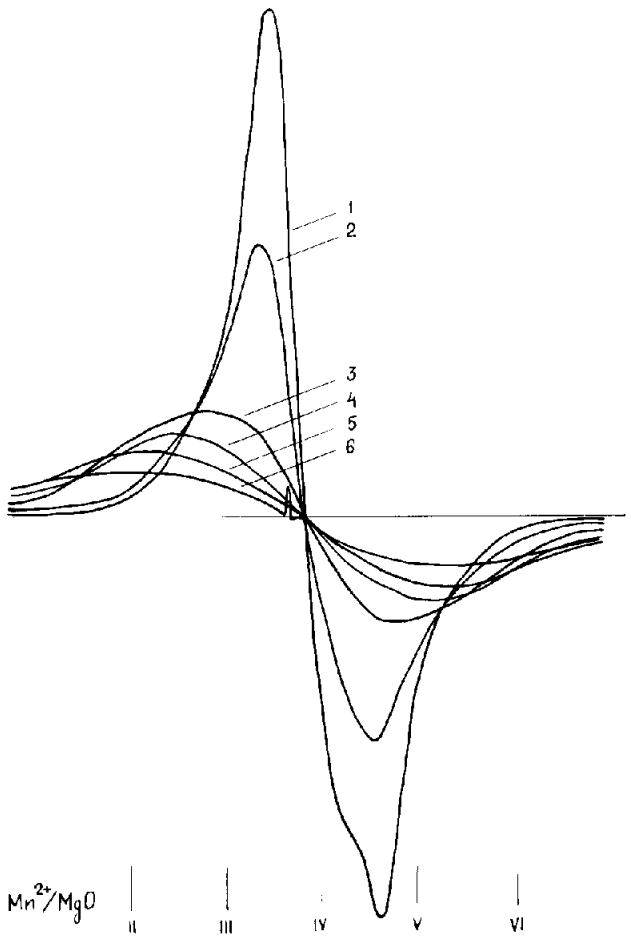

Fig. 9. ESR spectra of K_3CrO_8 at different stages of the induction period at 403 K (signals are 5-fold magnified against initial ones). 1, 2, 3, 4, 5 and 6 represent 10, 20, 30, 40, 50 and 60 min of heating, respectively.

ing in the ESR spectrum and to decreasing of signal intensity, are later considered in a generalized form as the formation of crystal lattice defects. Defects and microstresses are also observed with the help of X-ray diffraction: diffraction maxima are broadening, thus, leading to the merging of neighbouring reflexes (Fig. 12).

A narrow signal appears after the formation of thermolysis products in the course of decomposition. As to its properties, the signal is similar to the ESR spectrum of matrix-isolated CrO_8^{3-} ions that may be captured by crystal thermolysis products.

The reported data indicate profound changes in salt lattice at the stage of induction period of K_3CrO_8 decomposition which takes place in the entire crystal volume.

The product of complete thermal decomposition of K_3CrO_8 provides the

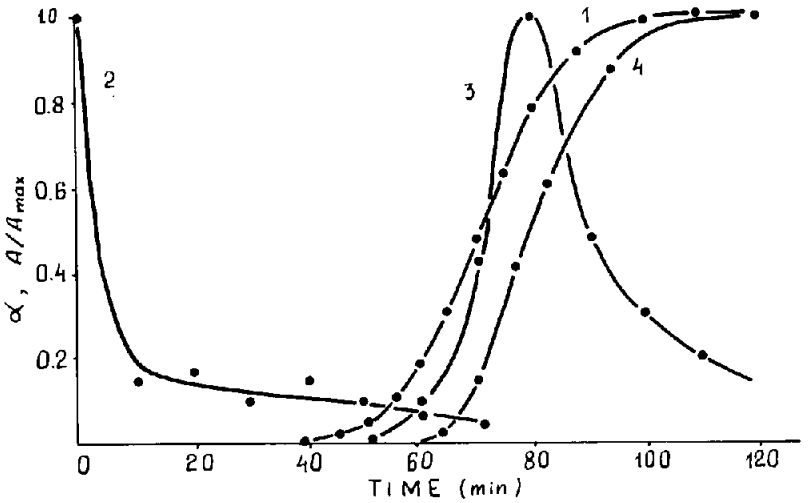

Fig. 10. Variation of the number of different paramagnetic centres (relative units): 1, kinetic curve of K_3CrO_8 thermolysis at 403 K; 2, CrO_8^{3-}; 3, matrix-isolated CrO_8^{3-}; 4, ion-radicals O_2^-.

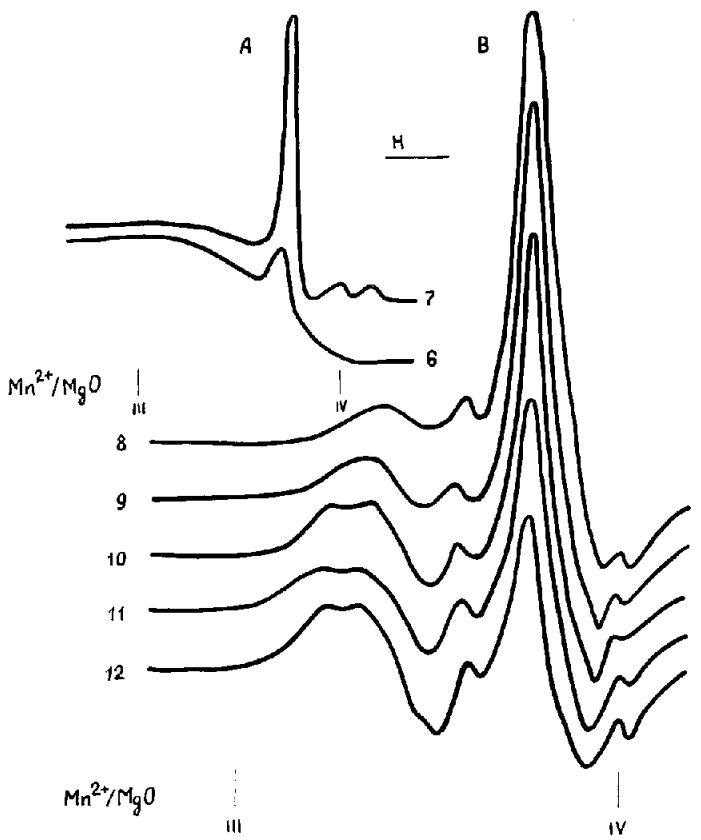

Fig. 11. ESR spectra of K_3CrO_8 in the intensive decomposition period (B signals are twice magnified compared to A signals); 6, 7, 8, 9, 10, 11 and 12 represent 60, 70, 80, 90, 100, 110 and 120 min of heating, respectively.

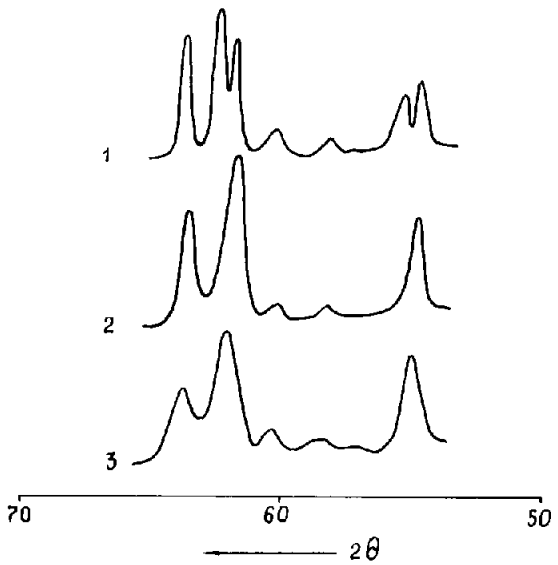

Fig. 12. K_3CrO_8 roentgenogram segments (1) with typical changes after heating corresponding to the middle of the induction period (2) and γ-irradiation of 88×10^6 r (3).

complex ESR spectrum in Fig. 13. This spectrum contains at least two lines, one of them corresponding to paramagnetic centres with a rhombic symmetry of the *g*-factor tensor. Basic values of the *g*-factor for this line are $g_1 = 2.027$; $g_2 = 2.009$; $g_3 = 2.002$. For better resolution, this spectrum is recorded by a device with the test wavelength $\lambda = 2.6$ cm. The small width of an individual line (about 5 Oe) indicates that paramagnetic centres are in a highly diluted state. They appear for the first time at $\alpha = 0.1$, reaching a maximum at $\alpha = 1$ (Figs. 10 and 11). It is most likely that these centres are O_2^- ion-radicals in the crystal matrix. Formation of O_2^- corresponds to the above scheme of K_3CrO_8 thermal decomposition.

In accordance with the received data, K_3CrO_8 thermolysis may be represented in the following way. As early as in the induction period with an observed slight gas release, K_3CrO_8 is essentially activated due to total formation of lattice defects. The formation of defects is accompanied by weak decomposition of the substance initiated by pioneer nuclei (biographic admixture of K_2CrO_4). This decomposition creates microstresses in the crystal, which results in the generation of dislocations; their motion and interaction with point defects leading to further nucleation. The latter may be regarded as evolution of the nuclei following the chain mechanism. This, however, involves the activation of diffusion processes in crystals, which is indirectly evidenced by the presence of matrix-isolated paramagnetic ions in them. Diffusion may initiate nucleation by the Hill mechanism [19]. Thus, chain and diffusion nucleation appear to be inseparably linked. An important factor is that the reaction is spreading quickly thanks to a high

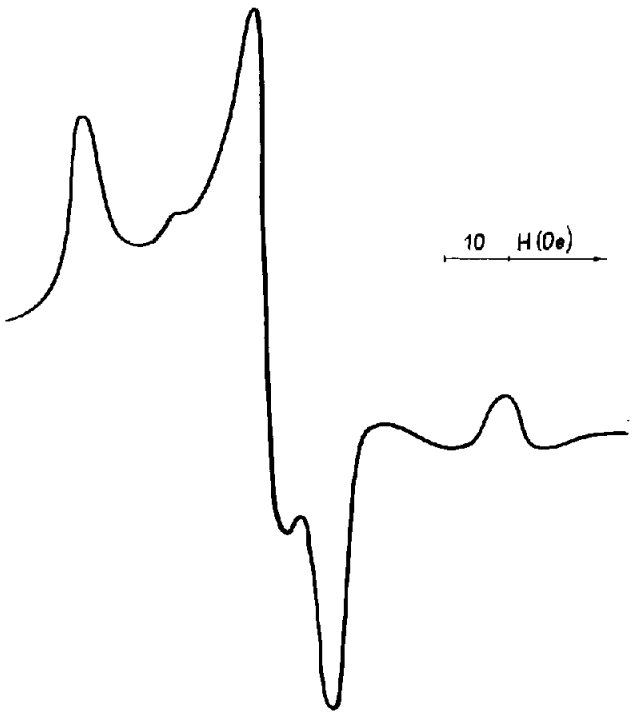

Fig. 13. ESR spectrum of K_3CrO_8 thermolysis products (λ = 2.6 cm).

concentration of defects in the salt crystal which appear in the induction period and highly activate the mass of the nondecomposed substance. The activating role of the defects formed in the induction period is taken into account insufficiently in the kinetics of topochemical processes, although it is the presence of these defects that may predetermine the development of the process following the mechanism of chain nucleation which, in a majority of cases, is considered from abstract and often uncertain positions [20].

The mechanism of K_3CrO_8 decomposition under discussion assumes an important contribution of the processes in the bulk of this substance. Additional experiments were performed to elucidate the role of surface reactions.

Preliminary irradiation of K_3CrO_8 by ultraviolet light in vacuum and in air somewhat shifts the kinetic curve (Fig. 14). The effect of γ-radiation is similar, but its large doses lead to complete disappearance of the rate increase length (Fig. 15). The difference between these kinds of radiation is that photolysis takes place on the crystal surface mainly, while radiolysis penetrates into the volume of crystals as well [10,21–23]. Therefore, large doses of γ-radiation lead to the same effect as preheating during the induction period (Fig. 12), and the rate increase length disappears. It is noteworthy that keeping irradiated salt in air, when thermolysis products (KO_2) decompose due to the interaction with H_2O vapour, leads to a

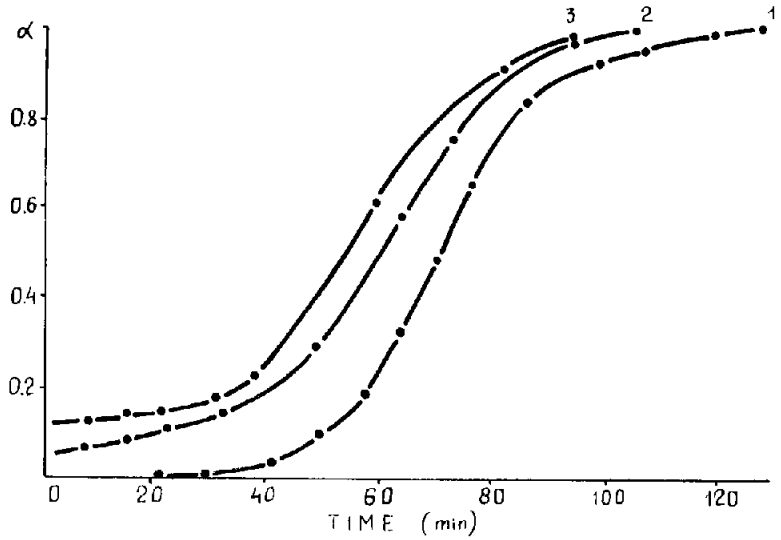

Fig. 14. Effect of preliminary irradiation with ultraviolet light on thermal K_3CrO_8 decomposition: 1, initial substance; 2, preliminary irradiated for 3 h; 3, irradiated for 3 h and kept in air.

situation at the beginning of thermolysis where the rate of the process during relatively long periods is lower compared to that of the newly irradiated samples (Figs. 14, 15). Retardation of the process was also observed after keeping a half-decomposed sample in air, but not in vacuum. Interrruptions

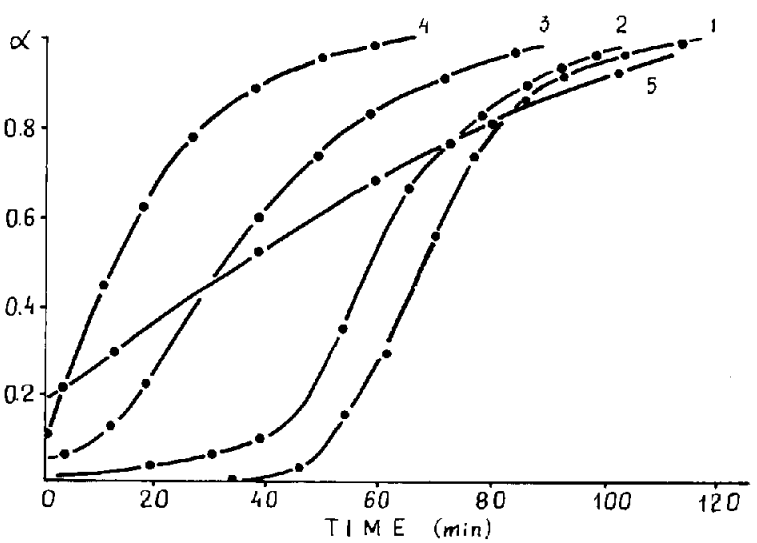

Fig. 15. Kinetic curves of thermal decomposition of γ-irradiated K_3CrO_8; 1, initial sample; 2, 3, 4, 11×10^6, 38×10^6 and 88×10^6 r, respectively; 5, 88×10^6 r, subsequently kept in air for 10 days.

in thermolysis in the middle and at the end of the induction period (both in vacuum and in air) do not noticeably affect subsequent decomposition. Thus, the changes on the sample surface have a strong effect on thermolysis only when the salt is enriched by defects and contains decomposition products (partly thermolysed and γ-irradiated substances). If the quantity of such products is small or they are absent but defects have already formed (samples obtained in the induction period of thermolysis) or if there are few defects and there are decomposition products (photolysed sample), then salt surface changes have little effect on thermolysis. These specificities may also be explained following the Hill mechanism [19] that assumes nucleation to be due to diffusion of the product to pre-nuclei, provided pre-nuclei are developing because of the defect formation in K_3CrO_8 crystals.

All these results manifest that potassium tetraperoxochromate (the most stable in the series of other tetraperoxochromates) is an interesting and perspective substance for further detailed investigation of the mechanism of topochemical reactions. The use of K_3CrO_8 for this aim seems to be preferable as compared to many other standard objects in topochemistry. As to K_3TaO_8 and K_3NbO_8 compounds, their thermolysis is characterized by the kinetics of monomolecular decomposition which is untypical of topochemical reactions [13]. This is probably due to the more simple stoichiometry of the decomposition of these salts ($K_3MO_4 + 2\ O_2$), impossible in the case K_2CrO_8 because of K_3CrO_4 instability.

ACKNOWLEDGEMENTS

The authors are grateful to V.M. Efremenkov, A.L. Poznyak and N.I. Zotov for their participation in some tests and discussions.

REFERENCES

1 W. Klemm and H. Werth, Z. Anorg. Allg. Chem., 216 (1933) 127.
2 R. Stomberg and C. Brosset, Acta Chem. Scand., 14 (1960) 441.
3 J.A. Ibers and J.D. Swalen, Phys. Rev., 127 (1962) 1914.
4 J.D. Swalen and J.A. Ibers, J. Chem. Phys., 37 (1962) 17.
5 J.E. Fergusson, C.J. Wilkins and J.F. Young, J. Chem. Soc., (1962) 2136.
6 W.P. Griffith, J. Chem. Soc., (1962) 3948.
7 B.R. McGarvei, J. Chem. Phys., 37 (1962) 2001.
8 J.W. Peters, J.N. Pitts, Jr., I. Rosenthal and H. Fuhr, J. Am. Chem. Soc., 94 (1972) 4348.
9 J.W. Peters, P.J. Bekowies, A.M. Winer and J.N. Pitts, Jr., J. Am. Chem. Soc., 97 (1975) 3299.
10 A.I. Lesnikovich, V.V. Sviridov and V.M. Efremenkov, Vestnik Byeloruss. Univ., Ser. II, (1974) N 3, 14.
11 N.S. Dalai, J.M. Millar, M.S. Jagadeesh and M.S. Seehra, J. Chem. Phys., 74 (1981) 1916.

12 A.I. Lesnikovich, A.L. Pozniak, V.V. Sviridov and K.K. Kovalenko, in Soveshanie po Kinetike i Mechanizmu Khimicheskih Reaksii v Tviordom Tele, Vol. 1, SO AN SSSR, Novosibirsk, 1977, p. 87.
13 G.V. Jere, L. Surendra and M.K. Gupta, Thermochim. Acta, 63 (1983) 229.
14 M.E. Brown, D. Dollimore and A.K. Galwey Reactions in the Solid State, Elsevier, Amsterdam, 1980.
15 G. Brauer, Handbook of Preparative Inorganic Chemistry, Vol. 2, Academic Press, New York, 1965.
16 V.S. Korolkov and A.K. Potapovich, Russ. Opt. Spektrosk., 16 (1964) 461.
17 E.H. Riesenfeld and H.F. Wohlers, Chem. Ber., 38 (1905) 1885.
18 C.P. Poole, Jr., Electron Spin Resonance, Comprehensive Treatise on Experimental Techniques, Wiley, New York, 1967.
19 R.A.W. Hill, Trans. Faraday Soc., 54 (1958) 685.
20 B. Delmon, Introduction a la Cinétique Hétérogéné, Technip, Paris, 1969.
21 V.V. Sviridov, Fotokhimiia i Radiacionnaia Khimiia Tviordih Neorganicheskih Veschestv, Visshaia Shkola, Minsk, 1964.
22 G.A. Branitskii, V.V. Sviridov and A.I. Lesnikovich, in Geterogennie Reaksii i Reaksionnais Sposobnost, Visshaia Shkola, Minsk, 1964, p. 149.
23 G.A. Branitskii and V.V. Sviridov, in Geterogennie Reaksii i Reaksionnais Sposobnost, Visshaia Shkola, Minsk, 1964, p. 166.